

# Green Bank Telescope Observations of the Eclipse of Pulsar “A” in the Double Pulsar Binary PSR J0737–3039

V. M. Kaspi,<sup>1,2,3</sup> S. M. Ransom,<sup>1,2</sup>  
D. C. Backer,<sup>4</sup> R. Ramachandran,<sup>4</sup> P. Demorest,<sup>4</sup> J. Arons,<sup>4,5</sup> A. Spitkovsky,<sup>6,5,7</sup>

## ABSTRACT

We report on the first Green Bank Telescope observations at 427, 820 and 1400 MHz of the newly discovered, highly inclined and relativistic double pulsar binary. We focus on the brief eclipse of PSR J0737–3039A, the faster pulsar, when it passes behind PSR J0737–3039B. We measure a frequency-averaged eclipse duration of  $26.6 \pm 0.6$  s, or  $0.00301 \pm 0.00008$  in orbital phase. The eclipse duration is found to be significantly dependent on radio frequency, with eclipses longer at lower frequencies. Specifically, eclipse duration is well fit by a linear function having slope  $(-4.52 \pm 0.03) \times 10^{-7}$  orbits  $\text{MHz}^{-1}$ . We also detect significant asymmetry in the eclipse. Eclipse ingress takes  $3.51 \pm 0.99$  times longer than egress, independent of radio frequency. Additionally, the eclipse lasts  $(40 \pm 7) \times 10^{-5}$  in orbital phase longer after conjunction, also independent of frequency. We detect significant emission from the pulsar on short time scales during eclipse in some orbits. We discuss these results in the context of a model in which the eclipsing material is a shock-heated plasma layer within the slower PSR J0737–3039B’s light cylinder, where the relativistic pressure of the faster pulsar’s wind confines the magnetosphere of the slower pulsar.

*Subject headings:* pulsars: general — pulsars: individual (PSR J0737–3039) — binaries: eclipsing — binaries: general — stars: neutron

---

<sup>1</sup>Department of Physics, Rutherford Physics Building, McGill University, 3600 University Street, Montreal, Quebec, H3A 2T8, Canada

<sup>2</sup>Department of Physics and Center for Space Research, Massachusetts Institute of Technology, Cambridge, MA 02139

<sup>3</sup>Canada Research Chair; NSERC Steacie Fellow

<sup>4</sup>Department of Astronomy, University of California, 601 Campbell Hall, Berkeley, CA 94720

<sup>5</sup>Theoretical Astrophysics Center and Physics Department, University of California, 601 Campbell Hall, Berkeley, CA 94720

<sup>6</sup>KIPAC, Stanford University, P.O. Box 20450, MS 29, Stanford, CA 94309

<sup>7</sup>Chandra Fellow

## 1. Introduction

The discovery of the double-pulsar binary system PSR J0737–3039 (Burgay et al. 2003; Lyne et al. 2004) represents a landmark in neutron-star astrophysics. This relativistic system consists of two neutron stars, both radio pulsars, in a 2.4-hr orbit having eccentricity 0.08, viewed nearly edge-on. The binary promises unparalleled tests of General Relativity. During each orbit, the faster-rotating of the two pulsars, PSR J0737–3039A (hereafter A), which has period  $P = 22$  ms, is eclipsed briefly at conjunction, while the slower-rotating of the two, PSR J0737–3039B ( $P = 2.7$  s; hereafter B), has unusual and longer-lived flux enhancements near the same epoch (Lyne et al. 2004). This bizarre and unprecedented behavior offers a new opportunity to understand pulsar magnetospheric and wind structures.

This paper is part of a short series describing the first follow-up observations of this remarkable source using the 100-m diameter National Radio Astronomy Observatory Green Bank Telescope (GBT).<sup>1</sup> Here we concentrate on the properties of the pulsar “A” eclipse. From observations at the Parkes and Lovell Telescopes, Lyne et al. (2004) have already established that the eclipse has duration 20–30 s and is roughly independent of frequency. The greater sensitivity of the observations described here reveal that the eclipse duration is in fact slightly but significantly dependent on radio frequency, as well as demonstrate for the first time that the eclipse is asymmetric.

## 2. Observations

Our observations with the GBT were promptly scheduled as a NRAO Rapid Response Science Program<sup>2</sup> four times in 2003 December and once in 2004 January and made use of receivers at 427, 820 and 1400 MHz. The observational details are summarized in Table 1. The 427 and 820 MHz receivers were located at the prime focus of the GBT, are cooled FET amplifiers, and have approximate system temperatures of 57 K and 25 K, respectively. The 1400 MHz receiver was located at the Gregorian focus and is a cooled HFET amplifier with system temperature of 20 K. All provide one beam and are sensitive to orthogonal polarizations. Signals from the receivers are transferred from the telescope to the control room via optical fibre.

The data reported on here were acquired with a single Berkeley-Caltech Pulsar Machine

---

<sup>1</sup>The National Radio Astronomy Observatory is a facility of the National Science Foundation operated under cooperative agreement by Associated Universities, Inc.

<sup>2</sup><http://www.vla.nrao.edu/astro/prop/rapid/>

(BCPM). The BCPM is an analog/digital filter bank which samples  $2 \times 96$  channels using 4 bits at flexible sampling rates and channel bandwidths (Backer et al. 1997). For our observations, the two orthogonal polarizations were summed in hardware prior to being written to disk. The sampling time for all observations was  $72 \mu\text{s}$ . The total bandwidth used (and hence the channel bandwidth) depended on the observing frequency (Table 1).

### 3. Analysis and Results

The data were analyzed using the PRESTO software package (Ransom 2001). We dedispersed the data using dispersion measure  $48.9115 \text{ pc cm}^{-3}$  and did the following analysis on the resulting time series. First, we folded data obtained within 2 min of pulsar A’s eclipse with the ephemeris reported by Lyne et al. (2004) using 64 phase bins. The resulting profile was cross-correlated with a high signal-to-noise template (obtained using data from several complete orbits at the appropriate radio frequency) and the temporal offset was recorded. Then, we folded data from within the 2 min of the eclipse again, but in 2-s intervals. We then determined the pulsed intensity in each 2-s interval, first by aligning the pulse with the template using the previously recorded offset, then by finding the best-fit scale factor between the template and aligned data profile. The best-fit value was found by  $\chi^2$  minimization, and the equivalent  $1\sigma$  uncertainties determined from the values of the scale factor corresponding to the minimum  $\chi^2$  plus 1. Note that no effort was made to calibrate the intensities in physical units; we assume that the telescope gain and system temperatures were constant throughout each observation. The average pulse arrival time in each 2-s interval was recorded and reduced to the solar system barycenter using the published position for the pulsar (Lyne et al. 2004). In this way, we obtained a pulsed flux intensity time series consisting of a barycentric time and an intensity for each of the 120 2-s intervals around conjunction. The number of conjunctions observed at each frequency is given in Table 2. Note that we found no evidence for any changes in dispersion measure near eclipse. Using the 427 MHz data, we set an upper limit on any dispersion-measure variation on  $\gtrsim 2$ -s time scales of  $0.016 \text{ pc cm}^{-3}$ . This was done by running the pulsar timing software package TEMPO<sup>3</sup> on the 427 MHz data (with eclipse points identified by large arrival-time uncertainty and omitted) without fitting for any parameters, and taking the largest residual as an upper limit on any delay due to an anomalous dispersion-measure change.

Average eclipse light curves for each frequency were obtained by combining results of every observed conjunction and are shown in Figure 1. The light curve at 427 MHz has more

---

<sup>3</sup><http://www.atnf.csiro.au/research/pulsar/timing/tempo/>

scatter than the other light curves, primarily due to higher levels of sporadic, short-time scale radio interference of unknown origin, particularly during the first orbit.

We detect significant variations in the pulsed emission at the same orbital phase but in different orbits, during the eclipse. An example of such variability is illustrated in Figure 2, in which the light curves for the three 1400 MHz eclipses are shown. In the second observed orbit, there is an apparent  $5\sigma$  detection of the pulsar during the nominal eclipse period, as indicated in the Figure. Investigation of this 2-s interval’s folded profile by eye confirmed that the pulse, with the expected pulse shape and phase (though appropriately noisy), was present (see Fig. 2, inset). Also, in Figure 1, there is emission in the eclipse region both before and after conjunction in the average 427 MHz light curve. Examination by eye confirmed the approximate pulse shape at the expected phase in several individual 2-s intervals in two of the three 427 MHz orbits. No such pulse appearance was seen in any of the 820 MHz eclipses, however.

Several new properties of the eclipse are apparent from Figure 1. First, the eclipse is clearly asymmetric in that the eclipse ingress is longer in duration than egress. Also, the eclipse appears to last longer post conjunction.

To quantify these properties, we fit the orbit-averaged light curves at each frequency with two functions of the form

$$F(\phi) = \frac{1}{e^{(\phi-\phi_0)/w} + 1}. \quad (1)$$

Here  $F(\phi)$  is the flux at orbital phase  $\phi$ , defined such that conjunction is at  $\phi = 0$ . This function, having two free parameters  $\phi_0$  and  $w$ , has value unity for  $(\phi - \phi_0)/w \ll -1$ , zero for  $(\phi - \phi_0)/w \gg 1$ , and one half for  $\phi = \phi_0$ . The transition from values near unity to zero occurs in a width  $\sim 2w$ . Optimal values of  $\phi_0$  and  $w$  for eclipse ingress and egress were determined separately for each light curve in Figure 1 using straightforward  $\chi^2$  minimization and data in the interval  $-0.006 < \phi < 0$  for ingress and  $0 < \phi < 0.006$  for egress. With two free parameters per side, the number of degrees of freedom per fit,  $\nu$ , was 23. The best fits are shown as solid curves in Figure 1; they generally yield values of reduced  $\chi^2$  near unity, except for the 427 MHz light curve, for which the higher  $\chi^2$  results from the extra scatter noted above. Contours of constant  $\chi^2$  in  $\phi_0/w$  space were approximately circular, indicating that these parameters were largely independent. Best-fit parameters and  $\chi^2_\nu$  values are given in Table 2.

Figure 3 summarizes the results of these fits. Panel (a) shows the eclipse FWHM, defined as the sum of ingress and egress values of  $|\phi_0|$ . The clear trend in the data indicates that the eclipse duration is frequency-dependent. Indeed the reduced  $\chi^2$  of a fit to the data assuming a simple constant mean value is 6.1, clearly ruling this model out. The data

are very well fit by a linear model, having slope  $(-4.52 \pm 0.03) \times 10^{-7}$  orbits  $\text{MHz}^{-1}$ , and intercept  $(3.412 \pm 0.003) \times 10^{-3}$ . This predicts that the eclipse will disappear at approximately 7.5 GHz, assuming no other eclipse mechanism becomes important. The mean eclipse FWHM duration, averaged over these three frequencies, is  $0.00301 \pm 0.00008$  in orbital phase, or  $26.6 \pm 0.7$  s.

Figure 3, panel (b), shows ingress and egress values of  $w$ . One aspect of the asymmetry of the eclipse is very apparent from this plot: all ingress values of  $w$  are higher than the egress values. Thus, the pulsar exits eclipse faster than it enters. We quantify this effect by taking the ratio of the ingress to egress values of  $w$ ,  $w_i/w_e$ . We find, for 427, 820 and 1400 MHz,  $w_i/w_e = 3.34 \pm 0.59, 3.74 \pm 0.78$ , and  $3.45 \pm 1.40$ , respectively. Thus, this aspect of the eclipse asymmetry is not dependent on frequency. The mean  $w_i/w_e$  is 3.51; the uncertainty on this value, estimated from the uncertainties at each frequency, is 0.99. Estimating the uncertainty from the RMS scatter in the three values suggests a much smaller uncertainty of 0.15; this may be a chance occurrence due to small-number statistics.

Figure 3, panel (c), shows the fitted values of  $\phi_0$  for ingress and egress at each frequency. Clearly,  $|\phi_0|$  values for egress are systematically larger than for ingress (Fig. 2c), demonstrating that the eclipse lasts longer post-conjunction. Note that the latter is *opposite* to what would be expected if the  $w$  asymmetry were the only one present, and hence is a different effect. We quantify this using the difference between ingress and egress values of  $\phi_0$ . For 427, 820 and 1400 MHz, we find differences of  $0.00042 \pm 0.00007$ ,  $0.00036 \pm 0.00006$ , and  $0.00042 \pm 0.00009$ , respectively. Thus we find no evidence for frequency dependence of this eclipse asymmetry. That the absolute values of  $\phi_0$  for both ingress and egress decrease significantly with increasing frequency is a restatement of the fact that the eclipse duration decreases with increasing frequency.

#### 4. Discussion

The best-fit inclination angle of the system as reported by Ransom et al. (2004) is  $88.7^\circ \pm 0.9^\circ$ . Given the measured projected semi-major axis of pulsar A’s orbit, this implies that A’s beam must pass within 0.07 lt-s of pulsar B. The latter has light-cylinder radius  $R_{lc} = cP/2\pi = 0.45$  lt-s. Thus, if B’s magnetosphere were unperturbed, then A’s beam as observed by us would have passed well within its light cylinder and through its magnetosphere. However, as discussed by Lyne et al. (2004), given the relative spin-down luminosities of the two pulsars, with A’s being a factor of  $\sim 3625$  greater than B’s, it seems inevitable that A’s wind has disrupted B’s outer magnetosphere at least halfway inside B’s light cylinder and possibly further out than A’s beam passes at conjunction. At A’s conjunction, the relative

transverse velocities of the pulsars is  $680 \text{ km s}^{-1}$ , so the eclipse duration implies an approximately constant physical size of the eclipsing region of 18,100 km, or 0.060 lt-s, comparable to the estimated 0.07 lt-s impact parameter, though in a direction parallel to the orbital plane. This clearly implies an eclipse region that is much smaller than B’s unperturbed magnetosphere.

Synchrotron absorption in a shock heated “magnetosheath” surrounding and containing B’s magnetosphere is a possible model for the A eclipse (Arons et al. 2004a; Lyutikov 2004, Arons et al., in preparation). A’s wind probably confines B’s magnetosphere on the side facing A (which changes periodically with B’s rotation over 2.7 s) such that the latter likely resembles a time-dependent variant of the Earth’s magnetosphere: compressed on the side facing the source of the wind (the Sun in the terrestrial case, A in this case) with a magnetotail on the opposite side. The plasma from A passes through a bow shock which spreads and weakens with distance down the flanks of the tail. The wind plasma from A which passes through the bow shock, flows in a magnetosheath layer between the bow shock and the magnetopause current layer that confines B’s magnetosphere. If the bow shock compresses and heats the A pulsar’s wind plasma as if it occurred in a weakly magnetized, semi-infinite flow, then synchrotron absorption in this shock heated plasma can account for the strong eclipse of A by B, albeit for surprisingly high pair densities in A’s wind (Arons et al. 2004a). The dimensions of the magnetopause and bow shock on the side facing A, along with the impact parameter of the line-of-sight with respect to B at conjunction, are such that A’s radio beam can pass through the northernmost or southernmost extremities of the magnetosheath layer (where north or south means with respect to the orbital plane.)

Such a scenario is consistent with the sharp edge and mildly frequency-dependent shape of the eclipse, since the synchrotron absorption optical depths at the observation frequencies used in this study are large and the shock causes the plasma density and relativistic temperature to jump up sharply across the thin shock layer. The eclipse-to-eclipse variations and occasional appearances of the pulse during the nominal eclipse region suggest a changing eclipse medium. If pulsar B is an oblique rotator, it is possible that the rotation of its magnetosphere causes the magnetospheric and bow shock shapes to be asymmetric on average between ingress and egress by amounts which account for the observed asymmetries.

If this picture and physical model is correct, one reaches the interesting conclusion that A’s wind shocks as if it is not strongly magnetized at a distance of only  $\sim 750$  times its light cylinder radius. Previous conclusions regarding pulsar wind magnetization have been derived from the behavior of relativistic winds as they pass through their termination shocks in pulsar wind nebulae (see Kaspi et al. 2004, for a recent review), located at much larger distances (typically  $\sim 10^7$  light cylinder radii) from their driving pulsars (e.g. Kennel &

Coroniti 1984).

The above A eclipse model (see Arons et al., in preparation) predicts that at sufficiently high radio frequencies, the eclipse will clear, consistent with the observed frequency dependence of the eclipse duration. For nominal, highly simplified models, transparency might appear at frequencies above 5–10 GHz, roughly quantitatively consistent with the observed frequency dependence extrapolation. If the impact parameter of the line-of-sight with respect to B during eclipse is sufficiently small, cyclotron scattering within B’s magnetosphere might also contribute to the high-frequency opacity. However, nominal values for the geometry suggest this to be unlikely. In addition, the eclipse duration and morphology should change with time on few-year time scales as relativistic periastron precession, and, perhaps more importantly, geodetic precession, which is expected to be very important in this system (Lyne et al. 2004), change the alignment of the pulsars. This will alter both our viewing vantage point and the dynamic pressure of A’s wind on B at conjunction.

The durations of pulsar A ingress and egress are comparable to the rotational period of B. As B’s magnetosphere could well present a different response to A’s wind pressure depending on B’s rotational phase, significantly different A eclipse behavior from orbit to orbit might be expected. A higher time resolution investigation with higher sensitivity may reveal B phase dependent effects on the eclipse.

We pay tribute to the Parkes survey team for so wonderful a discovery. We thank C. Bignell, F. Ghigo, and G. Langston for assistance with the GBT observations, and M. Roberts and B. Rutledge for useful discussions. This work was funded by an NSERC Discovery Grant and Steacie Fellowship Supplement to V.M.K. Additional funding to V.M.K. was provided by FQRST and CIAR. J.A. was partially supported by NASA grants TM4-5005X, NAG5-12031, G03-4063B and HST-HF-01157.01-A. He also thanks the taxpayers of California for their continued indulgence. A.S. acknowledges support provided by NASA through Chandra Fellowship PF2-30025 awarded by the Chandra X-ray Center, which is operated by the Smithsonian Astrophysical Observatory for NASA under contract NAS8-39073.

*Note added in proof.* – Very recently, McLaughlin et al. (2004) report modulation of A’s flux at B’s period during eclipse ingress, from a higher time resolution analysis of the 820 MHz data set used here. This suggests that the eclipse medium is indeed highly dependent on B’s rotational phase.

## REFERENCES

- Arons, J., Spitkovsky, A., Backer, D. C., Kaspi, V. M. 2004, in Proc. 2004 Apsen Winter Conf. on Astrophysics, “Binary Radio Pulsars,” eds. F. Rasio & I. Stairs, PASP, in press (astro-ph/0404159)
- Backer, D. C., Dexter, M. R., Zepka, A., D., N., Wertheimer, D. J., Ray, P. S., & Foster, R. S. 1997, PASP, 109, 61
- Burgay, M., D’Amico, N., Possenti, A., Manchester, R. N., Lyne, A. G., Joshi, B. C., McLaughlin, M. A., Kramer, M., Sarkissian, J. M., Camilo, F., Kalogera, V., Kim, C., & Lorimer, D. R. 2003, Nature, 426, 531
- Kaspi, V. M., Roberts, M. S. E., & Harding, A. K. 2004, in Compact Stellar X-ray Sources, ed. W. H. G. Lewin & M. van der Klis (United Kingdom: Cambridge University Press), in press
- Kennel, C. F. & Coroniti, F. V. 1984, ApJ, 283, 694
- Lyne, A. G., Burgay, M., Kramer, M., Possenti, A., Manchester, R. N., Camilo, F., McLaughlin, M. A., Lorimer, D. R., D’Amico, N., Joshi, B. C., Reynolds, J. R., & Freire, P. C. C. 2004, Science, 303, 1153
- Lyutikov, M. 2004, MNRAS, submitted (astro-ph/0403076)
- McLaughlin, M. A., et al. 2004, ApJ, submitted (astro-ph/0408297)
- Ransom, S. M. 2001, PhD thesis, Harvard University
- Ransom, S. M., Kaspi, V. M., Ramachandran, R., Demorest, P., Backer, D. C., Pfahl, E. D., Ghigo, F. D., & Kaplan, D. L. 2004, ApJ, 609, L71



Table 1: Summary of GBT Observations of PSR J0737–3039

Date (dd/mm/yy)	Start UTC	Start MJD	Duration (hr)	Frequency (MHz)	Bandwidth (MHz)	No. Channels
11/12/03	04:36:27	52984.19199	6.15	1400	96	96
18/12/03	04:12:15	52992.17519	5.30	820	48	96
23/12/03	05:22:22	52997.22388	4.72	820	48	96
01/01/04	03:30:09	53005.14595	6.22	427	48	96

Table 2: Fit Parameters for the PSR J0737–3039A Eclipse

Frequency (MHz)	No. Eclipses Observed	Ingress			Egress		
		$\phi_0$ ( $\times 10^{-3}$ )	$w$ ( $\times 10^{-3}$ )	$\chi_{23}^2$	$\phi_0$ ( $\times 10^{-3}$ )	$w$ ( $\times 10^{-3}$ )	$\chi_{23}^2$
427	3	$-1.60^{+0.05}_{-0.06}$	$0.56^{+0.06}_{-0.05}$	2.18	$1.82^{+0.03}_{-0.08}$	$0.17^{+0.03}_{-0.02}$	1.65
820	4	$-1.34^{+0.04}_{-0.05}$	$0.49^{+0.05}_{-0.04}$	0.834	$1.70^{+0.02}_{-0.03}$	$0.13^{+0.03}_{-0.02}$	0.76
1400	3	$-1.18^{+0.08}_{-0.06}$	$0.53^{+0.08}_{-0.08}$	0.53	$1.60^{+0.04}_{-0.04}$	$0.16^{+0.07}_{-0.06}$	1.02

Note:  $\chi_{23}^2$  is the reduced  $\chi^2$  for 23 degrees of freedom.

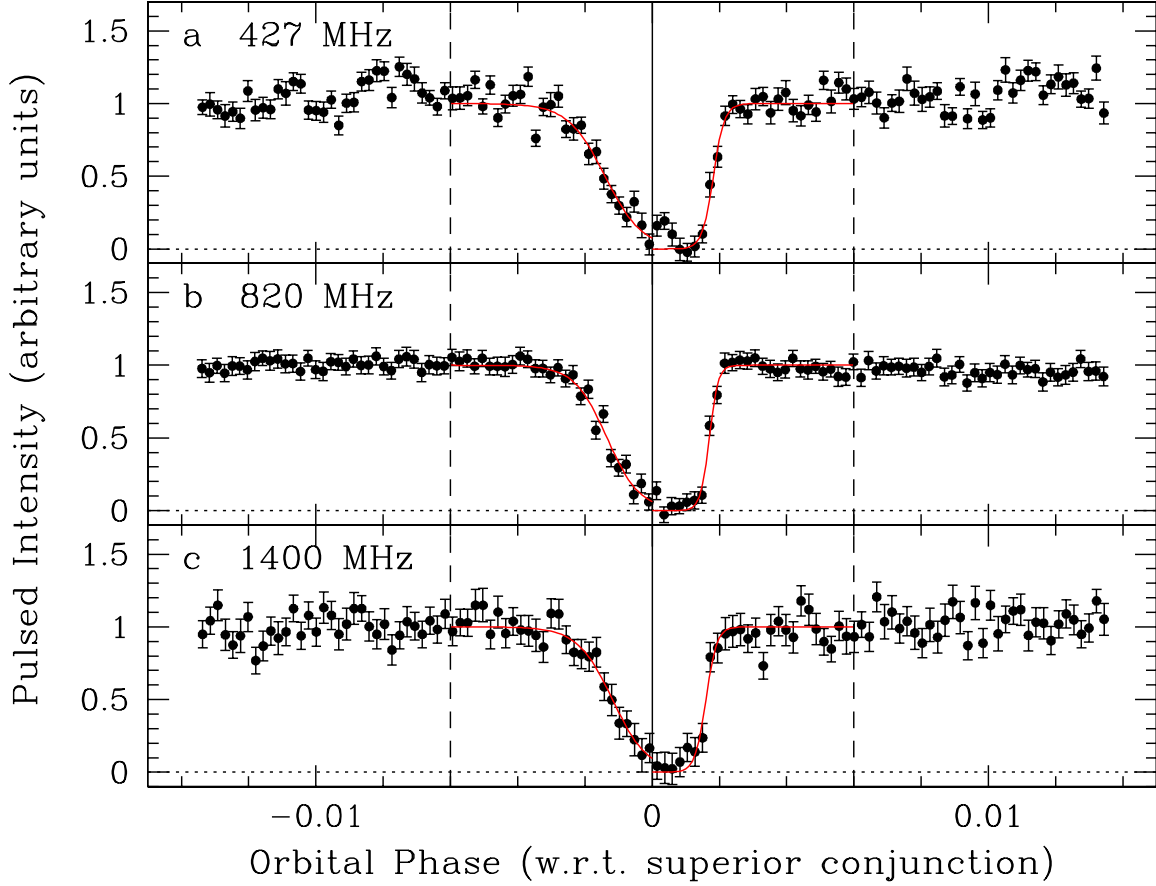


Fig. 1.— Pulsar A eclipse light curves. Each point represents 2 s of data; the shown curve is 4-min in duration, centered on conjunction. The x-axes are orbital phase with respect to conjunction. The y-axes are pulsed flux, normalized such that the pre-eclipse flux is unity. The panels are for (a) 427 MHz, (b) 820 MHz, and (c) 1400 MHz. The solid vertical line indicates conjunction and the horizontal dotted lines show 0 flux. Vertical dashed lines at  $\phi = -0.006, +0.006$  indicate the range of data fitted. The best-fit ingress and egress model curves are shown as solid lines. Best-fit parameters are provided in Table 2.

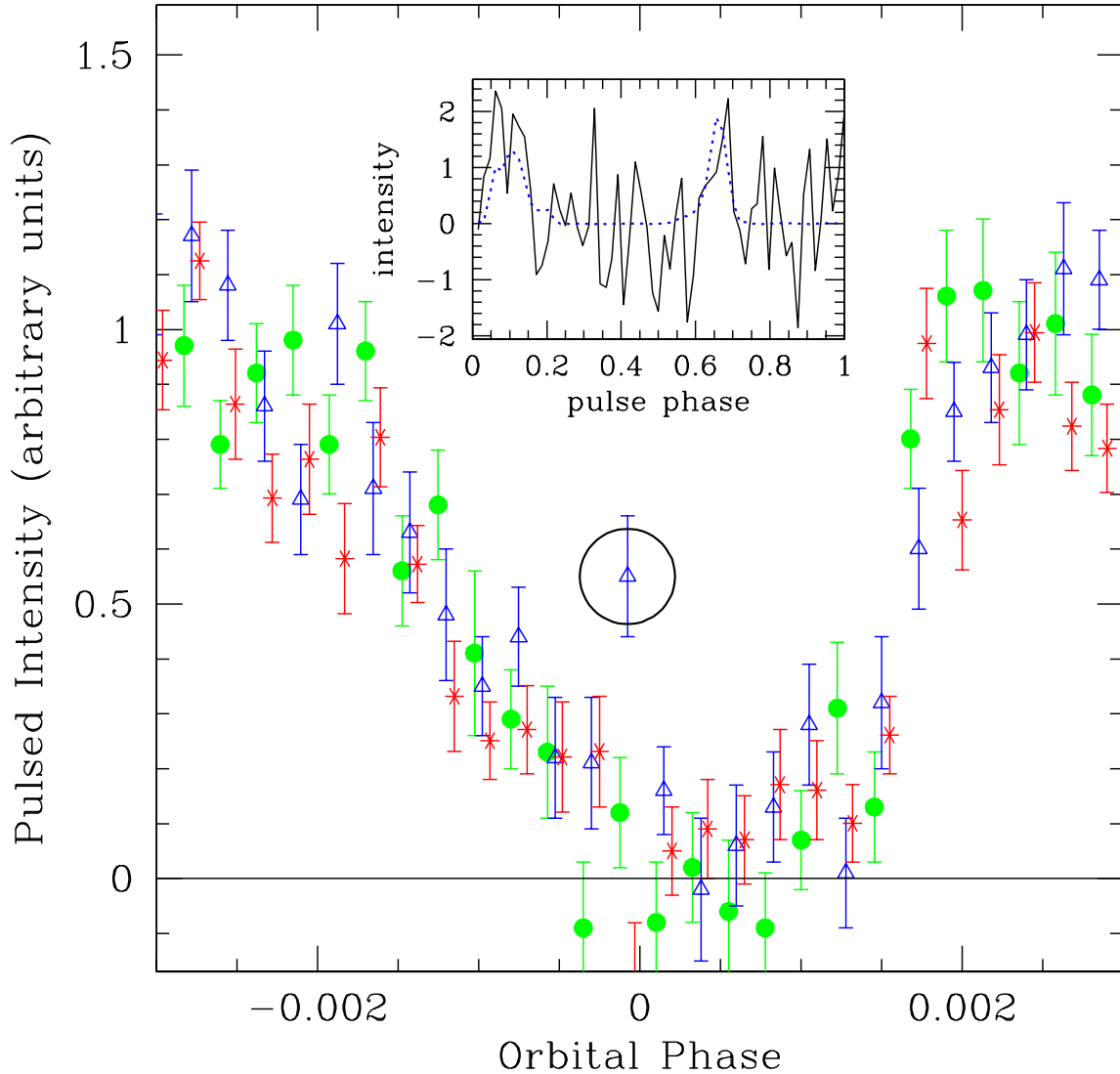


Fig. 2.— Close-up of eclipse region for the three orbits observed at 1400 MHz. The first, second and third orbits are indicated with circles, triangles and stars, respectively. Note the circled second orbit point just before conjunction; the pulsed intensity of this 2-s integration is  $5\sigma$  above zero, indicating significant pulsed emission during eclipse. The pulse profile for this 2-s interval is shown in the inset (solid line), as is the average template profile (dotted line), with the pre-determined phase alignment.

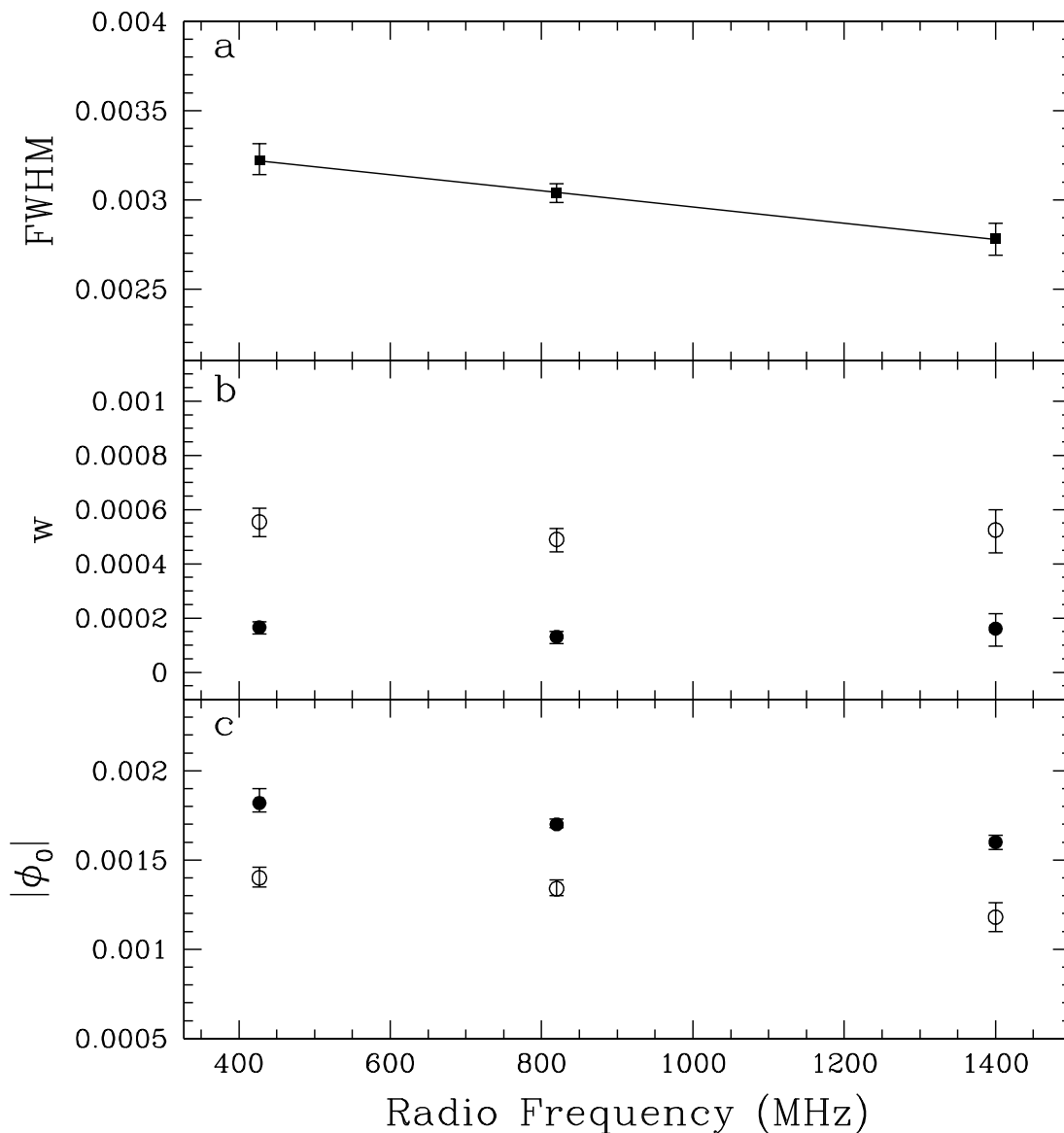


Fig. 3.— Various fitted properties of pulsar A’s eclipse as a function of radio frequency. Panel (a): eclipse duration (defined as the sum of the ingress and egress values of  $|\phi_0|$ , equivalent to FWHM), and best-fit linear model (solid line). Panel (b): values of  $w$  (approximately half the time for transition into and out of eclipse) for ingress (open symbols) and egress (filled symbols). Panel (c): values of  $|\phi_0|$  for ingress (open symbols) and egress (filled symbols).